

Zero-point-motion effects on the structure of C₆₀

Jorge Kohanoff,* Wanda Andreoni, and Michele Parrinello

IBM Research Division, Zurich Research Laboratory, CH-8803 Rüschlikon, Switzerland

(Received 12 May 1992)

The Car-Parrinello method and a new analysis procedure are used to determine the full vibrational spectrum of C₆₀. We evaluate the quantum effects on the structural properties of C₆₀ within the harmonic approximation. We find excellent agreement with the experimental pair correlation function. Zero-point-motion effects appear to be rather large.

While countless theoretical papers have been devoted to the determination of the structure and the vibrational properties of C₆₀, no effort has yet been made to our knowledge to calculate some of the experimentally determined quantities such as the pair correlation function $g(r)$ (Refs. 1 and 2) and the inelastic neutron scattering function $S(q, \omega)$,^{3,4} nor has the role of zero point motion been investigated. We shall do this here and shall observe that the role of the quantum fluctuations is rather large, namely, that zero-point-motion effects are essential to account for the experimental data. Calculation of quantum effects is greatly simplified by the harmonic assumption. Therefore, a necessary prerequisite to our evaluation is the detailed knowledge of all the vibrational eigenfrequencies and eigenmodes involved.

Several model calculations of the C₆₀ vibrational spectrum have been presented in the literature,⁵ but none has been based fully consistently on *ab initio* data. Very recently, some of us have performed an *ab initio* molecular-dynamics (MD) calculation based on the Car-Parrinello method,⁶ and generated a long trajectory for a C₆₀ molecule moving with classical dynamics, approximately equilibrated at a temperature of 450 K.⁷ The interatomic forces at each time step were calculated within the local-density approximation to density-functional theory. The calculation used pseudopotentials and a plane-wave expansion for the Kohn-Sham orbitals. A detailed account of the computational method can be found in Ref. 7.

The calculated equilibrium structure gave 1.45 and 1.39 Å for single and double bonds, respectively. In Ref. 7 an attempt was made to extract the harmonic frequencies from an analysis of the trajectories based on the multiple signal classification (MUSIC) analysis method.⁸ This attempt was only partially successful and just a few eigenmodes could be unambiguously assigned, since the signal-to-noise ratio was too unfavorable for the others. Very recently, one of us⁹ developed an improved MUSIC-based analysis algorithm that has been able to circumvent this difficulty and, from the very same data set, extract all the eigenfrequencies and eigenvectors.

We recall here that, contrary to conventional Fourier-transform methods, the MUSIC signal analysis can achieve resolutions in frequency higher than $2\pi/\tau$, where τ is the length of the MD run. Also the MUSIC frequency estimator exhibits peaks at the frequencies that are present in the spectrum, but the strength of these peaks is not proportional to their weight in the original data set. Thus, full thermal equilibration of the vibrational modes

is not necessary to observe the peaks in the MUSIC spectrum. It suffices that the mode be excited, even slightly. This is crucial since in highly harmonic systems it is very difficult and computationally costly to reach thermal equilibrium. However, some of the frequencies in the MUSIC spectrum in the presence of anharmonicity and/or short run, appear to move significantly when varying the sampling interval and/or the number of signals included in the analysis. This leads to the difficulties mentioned above.⁷

In order to solve this problem, we first perform a symmetry decomposition of the MD trajectory in the irreducible representations of the icosahedral group. In this way we improve the signal-to-noise ratio, as well as the number of frequencies to be extracted from the symmetrized trajectories, which is dramatically reduced. This greatly helps to stabilize the analysis but is not sufficient to resolve all the frequencies unambiguously. Thus we proceed as follows. We first estimate the frequencies with the MUSIC algorithm. Then we fit the symmetrized trajectories to linear combinations of eigenmodes at these frequencies. The amplitudes of the eigenmodes and the eigenvectors components are the fitting parameters. Orthogonality of the eigenvectors is enforced throughout the fitting procedure. Then, the trajectories are projected onto the estimated eigenvectors, and the MUSIC analysis is performed again. This forms the basis for a self-consistent refining of the frequencies, although in practice one or two iterations are enough. Moreover, the projection is a very robust test for the unstable signals, since if they represent noise, these signals disappear in the first iteration.

In Table I we present our results and compare them with the experimental frequencies of the optically active infrared (T_{1u}) and Raman ($A_g + H_g$) modes.¹⁰ The agreement is rather satisfactory, aside from a slight underestimation of the frequencies of the order of 3 meV. This can be ascribed to the local-density approximation and the limited energy cutoff used in the plane-wave expansion, since it is systematic and far beyond the error estimated for the data analysis method (~ 0.6 meV). The general quality of our results for the other frequencies can be judged by a comparison between the experimental inelastic neutron scattering spectrum, and the dynamical structure factor $S(q, \omega)$ theoretically determined, in the small- q limit, as¹¹

$$S(q, \omega) \propto q^2 \sum_{i=1}^{174} \langle u_i^2 \rangle \delta(\omega - \omega_i), \quad (1)$$

TABLE I. Calculated vibrational frequencies of C_{60} (in cm^{-1}). Infrared and Raman measured frequencies are quoted in parentheses. The error in the determination of the frequencies due to the data analysis method is estimated to be $\pm 5 \text{ cm}^{-1}$.

A_g^a	T_{1g}	T_{2g}	G_g	H_g^a	A_u	T_{1u}^a	T_{2u}	G_u	H_u
455 (496)	547	527	455	246 (273)	881	510 (527)	321	332	381
1365 (1470)	799	744	560	410 (437)		534 (570)	730	720	509
	1211	770	737	689 (710)		1092 (1170)	833	751	634
		1186	988	731 (774)		1320 (1407)	1045	886	725
			1240	1036 (1099)			1450	1216	1130
			1395	1140 (1250)				1316	1240
				1315 (1428)					1458
				1484 (1575)					

^aExperimental frequencies from Ref. 10.

where the sum runs over all the eigenfrequencies ω_i , and the average square amplitude of the i th mode is given by¹²

$$\langle u_i^2 \rangle = \frac{\hbar}{2m\omega_i} \coth \left(\frac{\hbar\omega_i}{2k_B T} \right). \quad (2)$$

We present the calculated values of $S(q, \omega)$ in Fig. 1, in comparison with the experimental data, for $\omega \leq 100 \text{ meV}$

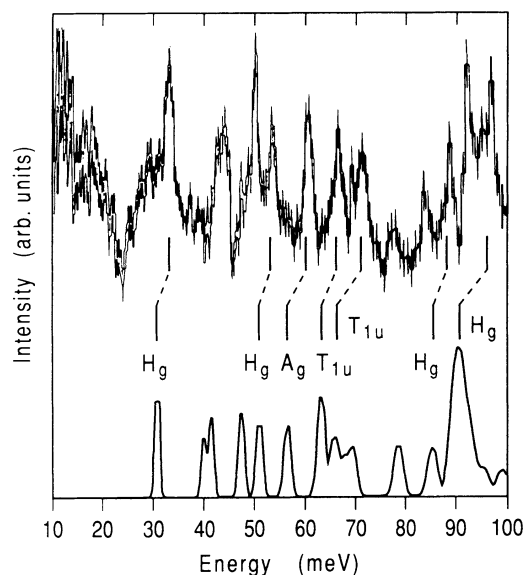


FIG. 1. Inelastic neutron scattering spectrum (upper curve, from Ref. 4) compared to the calculated dynamical structure factor $S(q, \omega)$ [Eq. (1), lower curve]. The broadening of the theoretical peaks has been generated by convoluting them with a Gaussian window of width $\Delta\omega/\omega = 1\%$. The upper part of the spectrum ($\omega > 100 \text{ meV}$) is avoided due to the lack of high-quality experimental data. The optically active infrared and Raman modes are identified in both curves and connected accordingly.

($1 \text{ meV} = 8.066 \text{ cm}^{-1}$). The data measured for $\omega > 100 \text{ meV}$ are rather confusing and, therefore, that part of the spectrum is avoided for the sake of clarity. The frequencies of the optically active modes are also shown and compared to the experimental ones.¹⁰ The general features of the C_{60} phonon spectrum have been discussed several times.⁵ Our calculation confirms what is already known. However, it might be stressed that contrary to other calculations¹³⁻¹⁵ and, in agreement with experiment, it does not present any significant gap in the vibrational density of

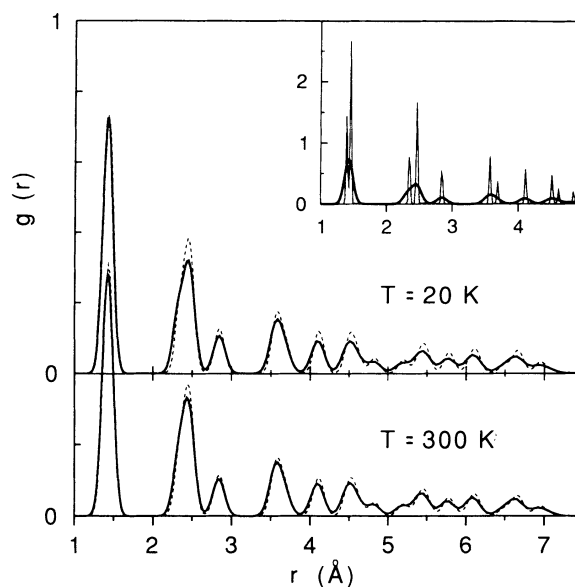


FIG. 2. Pair correlation function $g(r)$ at $T = 20$ and 300 K . Thick solid curves denote experimental data [2]. Dashed curves correspond to the present calculation, taking into account the *quantum* statistics. In the inset, we show the theoretical result using *classical* statistics (thin solid line), compared to experiment, at $T = 20 \text{ K}$. Note that, classically, the first peak is split.

states around 1100 cm⁻¹.

Having determined with good accuracy the eigenfrequencies and the corresponding eigenmodes, we are in the position to calculate structural properties within the quantum harmonic approximation. We shall focus on the calculation of the pair correlation function $g(r)$, for which there are very accurate experimental data available at $T=20$ and 300 K.² We express the pair correlation function as

$$g(r) = \sum_{i \neq j}^N \int \rho(\mathbf{r}_1, \dots, \mathbf{r}_N) \delta(r - |\mathbf{r}_i - \mathbf{r}_j|) d\mathbf{r}_1 \dots d\mathbf{r}_N, \quad (3)$$

where $\rho(\mathbf{r}_1, \dots, \mathbf{r}_N)$ is the *quantum* density matrix of the system, and the sum runs over all the particles. For a harmonic system the matrix $\rho(\mathbf{r}_1, \dots, \mathbf{r}_N)$ can be decomposed as a product of single-oscillator terms $\rho(u_i, \omega_i)$ provided that the u_i 's are the normal coordinates. The integral resulting from Eq. (3) has then been evaluated with a Monte Carlo method generating the $\{u_i\}$ randomly and independently, according to the Gaussian distribution:¹²

$$\rho(u_i, \omega_i) = \left(\frac{m\omega_i}{2\pi\hbar \sinh f_i} \right)^{1/2} \exp \left[-\frac{m\omega_i}{\hbar} u_i^2 \tanh f_i \right] \quad (4)$$

with $f_i = \hbar \omega_i / 2k_B T$.

We present our results for the $T=20$ K and the $T=300$ K cases in Fig. 2, in comparison to experimental data. The agreement between theory and experiment is very good. Most remarkable is the fact that in the first peak

the distinction between single and double bonds is completely absent due to zero point motion. In the inset we show the resulting pair correlation function, computed according to Boltzmann classical statistics at $T=20$ K. The detailed structure of the molecule and the single-bond double-bond splitting of the first peak is clearly visible, although unphysical. Our results do not imply that the average C₆₀ structure does not exhibit bond alternation. That they do so is confirmed by NMR,¹⁶ and x-ray,¹⁷ electron,¹⁸ and neutron¹⁹ diffraction data. The quantum fluctuations, however, are larger than bond separation. For instance, the root-mean-square vibration at $T=0$ K is given by $\langle (r_i - r_i^0)^2 \rangle^{1/2} \approx 0.044$ Å, comparable to the single-bond double-bond splitting of 0.06 Å.

The extent of the zero-point-motion effects, apparently unnoticed so far, is comparable in magnitude with Jahn-Teller splitting-induced displacements.²⁰ This can lead to substantial renormalization of the electron-phonon coupling. Reported calculations of electron-phonon coupling have not included this effect.²¹ Finally, we want to remark that quantum effects can also be very large in other fullerenes such as C₇₀. The recent claim²² that on the basis of experimentally determined $g(r)$ one can discriminate between different models is probably not well founded.

We thank W. I. F. David for providing us with the results of the experimentally determined pair correlation function prior to publication. One of us (J.K.) also acknowledges E. Tosatti and F. Gygi for helpful discussions.

*Corresponding author. BITNET address: JOK@ZURLVM1.

¹F. Li, D. Ramage, J. S. Lannin, and J. Conceição (unpublished).

²A. K. Soper, W. I. F. David, D. S. Sivia, T. J. S. Dennis, J. P. Hare, and K. Prassides, *J. Phys. Condens. Matter* (to be published).

³R. L. Cappelletti, J. R. D. Copley, W. A. Kamitakahara, Fang Li, J. S. Lannin, and D. Ramage, *Phys. Rev. Lett.* **66**, 3261 (1991).

⁴K. Prassides, T. J. S. Dennis, J. P. Hare, J. Tomkinson, H. W. Kroto, R. Taylor, and D. R. M. Walton, *Chem. Phys. Lett.* **187**, 455 (1991).

⁵See, e.g., F. Negri, G. Orlandi, and F. Zerbetto, *Chem. Phys. Lett.* **190**, 174 (1992), and references therein.

⁶R. Car and M. Parrinello, *Phys. Rev. Lett.* **55**, 2471 (1985).

⁷B. P. Feuston, W. Andreoni, M. Parrinello, and E. Clementi, *Phys. Rev. B* **44**, 4056 (1991).

⁸S. Lawrence Marple, Jr., *Digital Spectral Analysis with Applications* (Prentice-Hall, Englewood Cliffs, NJ, 1987).

⁹J. Kohanoff (unpublished).

¹⁰D. S. Bethune, G. Meijer, W. C. Tang, H. J. Rosen, W. G. Golden, H. Seki, C. A. Brown, and M. S. de Vries, *Chem. Phys. Lett.* **179**, 181 (1991).

¹¹A. D. B. Woods, B. N. Brockhouse, M. Sakamoto, and R. N. Sinclair, *Inelastic Scattering of Neutrons in Solids and Liquids* (IAEA, Vienna, 1961).

¹²R. P. Feynman, *Statistical Mechanics: A Set of Lectures* (Benjamin, Reading, MA, 1976).

¹³R. E. Stanton and M. D. Newton, *J. Phys. Chem.* **92**, 2141 (1988).

¹⁴G. B. Adams, J. B. Page, O. F. Sankey, K. Sinha, and J. Menéndez, *Phys. Rev. B* **44**, 4052 (1991).

¹⁵G. Onida and G. Benedek, *Europhys. Lett.* **18**, 403 (1992).

¹⁶C. S. Yannoni, P. P. Bernier, D. S. Bethune, G. Meijer, and J. R. Salem, *J. Am. Chem. Soc.* **113**, 3190 (1991).

¹⁷J. M. Hawkins, A. Meyer, T. A. Lewis, S. D. Loren, and F. J. Hollander, *Science* **252**, 312 (1991).

¹⁸K. Hedberg, L. Hedberg, D. S. Bethune, C. A. Brown, H. C. Dorn, R. D. Johnson, and M. S. de Vries, *Science* **254**, 410 (1991).

¹⁹W. I. F. David, R. M. Ibberson, J. C. Matthewman, K. Prassides, T. J. S. Dennis, J. P. Hare, H. W. Kroto, R. Taylor, and D. R. M. Walton, *Nature (London)* **353**, 147 (1991).

²⁰W. Andreoni and M. Parrinello (unpublished).

²¹See, e.g., R. A. Jishi and M. S. Dresselhaus, *Phys. Rev. B* **45**, 2597 (1992); M. Schlüter, M. Lannoo, M. Needels, G. A. Baraff, and D. Tománek, *Phys. Rev. Lett.* **68**, 526 (1992); C. M. Varma, J. Zaanen, and K. Raghavachari, *Science* **254**, 989 (1991).

²²D. R. McKenzie, C. A. Davis, D. J. H. Cockayne, D. A. Muller, and A.M. Vassallo, *Nature (London)* **355**, 622 (1992).